Dynamic Modeling and Analysis of a Double-Star Synchronous Machine Interfaced with a Static Converter

Mouhamed MBENGUE[1*], Abdoulaye DIENG[2]**

[1]PhD Student, Laboratory of Water, Energy, Environment and Industrial Processes (LE3PI)
Polytechnic School (ESP) – Cheikh Anta Diop University of Dakar (UCAD)
Fann, BP 5085, Dakar-Fann, Senegal
*mouhamed.mbengue@esp.sn

[2]Professor, PhD Supervisor, Department of Electrical Engineering
Polytechnic School (ESP) – Cheikh Anta Diop University of Dakar (UCAD)
Fann, BP 5085, Dakar-Fann, Senegal
**abdoulaye.dieng@esp.sn

Abstract–This paper presents a rigorous modeling of the "Double-Star Permanent Magnet Synchronous Machine – Static Converter" (DS-PMSM) system operating in generator mode. The model is based on Concordia and Park transformations to express electrical quantities in a rotating reference frame, thereby simplifying dynamic analysis. The double-star structure enables independent control of the two stator sets, optimizing energy production and the regulation of active (P) and reactive (Q) power. The static converter is modeled using a behavioral approach based on dual three-phase inverters. The fundamental equations (flux, voltage, torque) are developed in both *abc* and *dq* reference frames. This modeling framework provides a solid foundation for implementing robust control strategies and optimized energy injection into the grid.

Keywords–Double-star synchronous machine, DS-PMSM, dynamic modeling, static converter, dq transformations, grid injection

I. Introduction

Multiphasic synchronous machines, particularly the Double-Star Permanent Magnet Synchronous Machine (DS-PMSM), are receiving growing attention in renewable energy systems. Thanks to their two independent three-phase stator windings, they offer improved redundancy, enhanced fault tolerance, and greater flexibility for vector control and the regulation of active and reactive power.

This topology is particularly well-suited to applications requiring service continuity and optimal grid power injection. Efficient dynamic models have been proposed to facilitate control design, including the decoupled *dq* model introduced by Kallio *et al.* [1], and modeling comparisons conducted by Amirouche *et al.* [2].

Accurate and coupled modeling of the DS-PMSM and its static converter is a crucial step toward the development of robust control strategies. Such modeling makes it possible to anticipate electromechanical interactions and ensure optimal and stable power injection into the grid, particularly in highly variable environments. The decoupled *dq* model proposed by Andriollo *et al.* [3] clearly demonstrates the benefits of this approach for analyzing and designing efficient control systems.

This article establishes a comprehensive model of the DS-PMSM with its associated static converter, from the fundamental *abc*-frame equations to the transformed *dq*-form, incorporating realistic physical assumptions. It also includes a behavioral model of the two three-phase inverters.

II. Related Work

The early work by Maachou and Naami [4] introduced vector control applied to DS-PMSMs, using the Park transformation to manage the two stator windings independently. More recent studies, such as those by Zhou *et al.* [5] and Fakharudin *et al.* [6], extended this approach to permanent magnet generators by integrating robust strategies such as Direct Torque Control (DTC) and Field Oriented Control (FOC) for active and reactive power (P/Q) injection into the grid.

Kallio *et al.* [1] proposed a decoupled *dq* model to simplify the control design, while Amirouche *et al.* [2] compared several modeling techniques under degraded operating conditions. Finally, Andriollo *et al.* [3] and Naas *et al.* [7] demonstrated the relevance of differential control schemes to enhance fault tolerance and energy management in DS-PMSMs.

III. Methodology and Modeling

A. Modeling Assumptions

The proposed model is based on the following assumptions:

- Unsaturated magnetic circuit [8]
- Homogeneous air gap [9]
- Sinusoidal magnetic field distribution [10]
- Neglect of core losses and parasitic capacitances [8], [9], [11]
- Symmetrical stator windings [4], [12]
- Ideal permanent magnets [10]

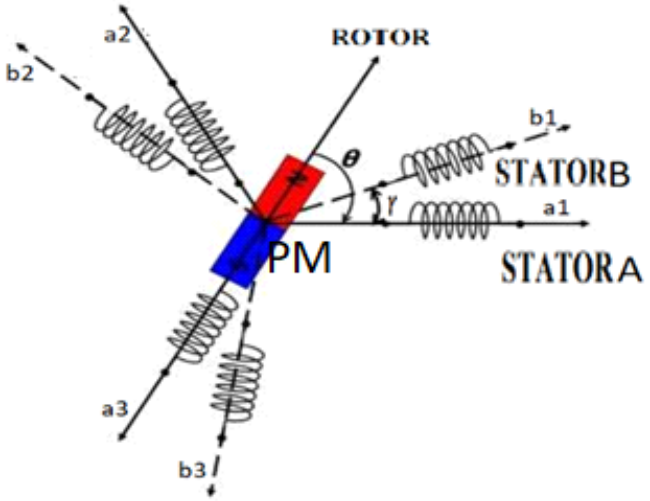

Fig. 1: Structure of a double-star permanent magnet synchronous machine, with the two stator windings A and B phase-shifted, and a magnetized rotor.

B. Dynamic Equations of the DS-PMSM

- Stator star A: $\{a_1, a_2, a_3\}$
- Stator star B: $\{b_1, b_2, b_3\}$
- Global set: $Y_i \in \{a_1, a_2, a_3, b_1, b_2, b_3\}$, $i \in \{1, 2, 3\}$
- $R = R_S$: stator phase resistance; $L = L_S = L_{d_Y} = L_{q_Y}$
- J: rotor inertia; $\omega_{mec}(t)$: mechanical speed; $C_r(t)$: load torque; f: viscous friction coefficient
- $\gamma = \dfrac{\pi}{6}$: electrical phase shift between stator stars A and B
- Rotor electrical position: $\theta = \theta_Y = \int \omega(t)\, dt + \theta_0$

1) In the abc Reference Frame (per stator star):

- **Flux:**

$$\varphi_{Y_i}(t) = L_s \cdot i_{Y_i}(t) + \varphi_{Y_i}^{PM}(t) \tag{1}$$

- **Voltage:**

$$v_{Y_i}(t) = R_S \cdot i_{Y_i}(t) + \frac{d\varphi_{Y_i}(t)}{dt} \tag{2}$$

- **Electromagnetic torque:**

$$C_{em}(t) = \sum_{i=1}^{3} i_{a_i}(t) \cdot \frac{d\varphi_{a_i}(t)}{d\theta} + \sum_{i=1}^{3} i_{b_i}(t) \cdot \frac{d\varphi_{b_i}(t)}{d\theta} \tag{3}$$

$$C_{em}(t) = C_{emA}(t) + C_{emB}(t) \tag{4}$$

$$C_{em}(t) = n_{pp} \cdot \varphi \cdot (i_{q_A}(t) + i_{q_B}(t)) \tag{5}$$

- **Mechanical dynamics:**

$$J \cdot \frac{d\omega_{mec}(t)}{dt} = C_{em}(t) - C_r(t) - f \cdot \omega_{mec}(t) \tag{6}$$

2) Three-phase to two-phase transformation: $R = R_S$, $L = L_S = L_{d_Y} = L_{q_Y}$, and $\varphi = \varphi_f = \varphi^{PM}$.

a) Concordia Transformation:

- **Reduced Direct Concordia (from** abc **to** $\alpha\beta$**):**

$$\begin{bmatrix} x_\alpha \\ x_\beta \end{bmatrix} = \sqrt{\frac{2}{3}} \begin{bmatrix} 1 & -\frac{1}{2} & -\frac{1}{2} \\ 0 & \frac{\sqrt{3}}{2} & -\frac{\sqrt{3}}{2} \end{bmatrix} \begin{bmatrix} x_a \\ x_b \\ x_c \end{bmatrix} \tag{7}$$

- **Reduced Inverse Concordia (from** $\alpha\beta$ **to** abc**):**

$$\begin{bmatrix} x_a \\ x_b \\ x_c \end{bmatrix} = \sqrt{\frac{2}{3}} \begin{bmatrix} 1 & 0 \\ -\frac{1}{2} & \frac{\sqrt{3}}{2} \\ -\frac{1}{2} & -\frac{\sqrt{3}}{2} \end{bmatrix} \begin{bmatrix} x_\alpha \\ x_\beta \end{bmatrix} \tag{8}$$

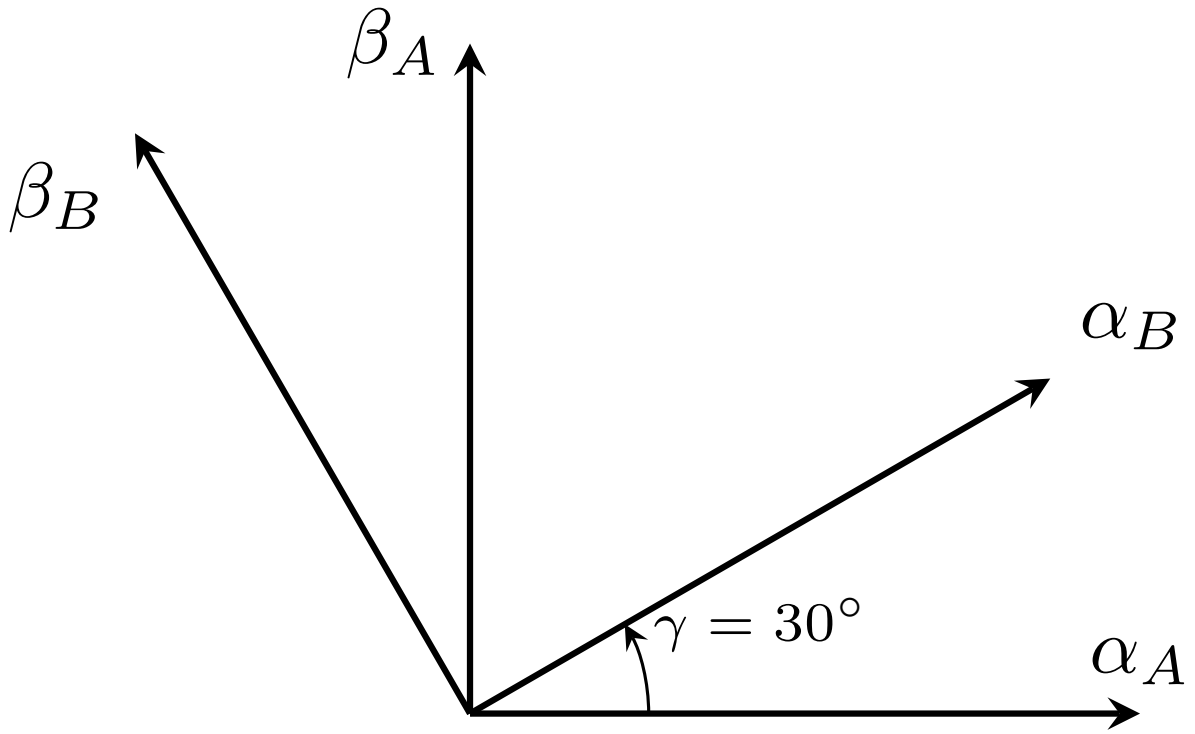

Fig. 2: Fixed two-phase reference frame.

b) Park Transformation:

- **Direct Park (from** $\alpha\beta$ **to** dq**):**

$$\begin{bmatrix} x_d \\ x_q \end{bmatrix} = \begin{bmatrix} \cos\theta & \sin\theta \\ -\sin\theta & \cos\theta \end{bmatrix} \begin{bmatrix} x_\alpha \\ x_\beta \end{bmatrix} \tag{9}$$

- **Inverse Park (from** dq **to** $\alpha\beta$**):**

$$\begin{bmatrix} x_\alpha \\ x_\beta \end{bmatrix} = \begin{bmatrix} \cos\theta & -\sin\theta \\ \sin\theta & \cos\theta \end{bmatrix} \begin{bmatrix} x_d \\ x_q \end{bmatrix} \tag{10}$$

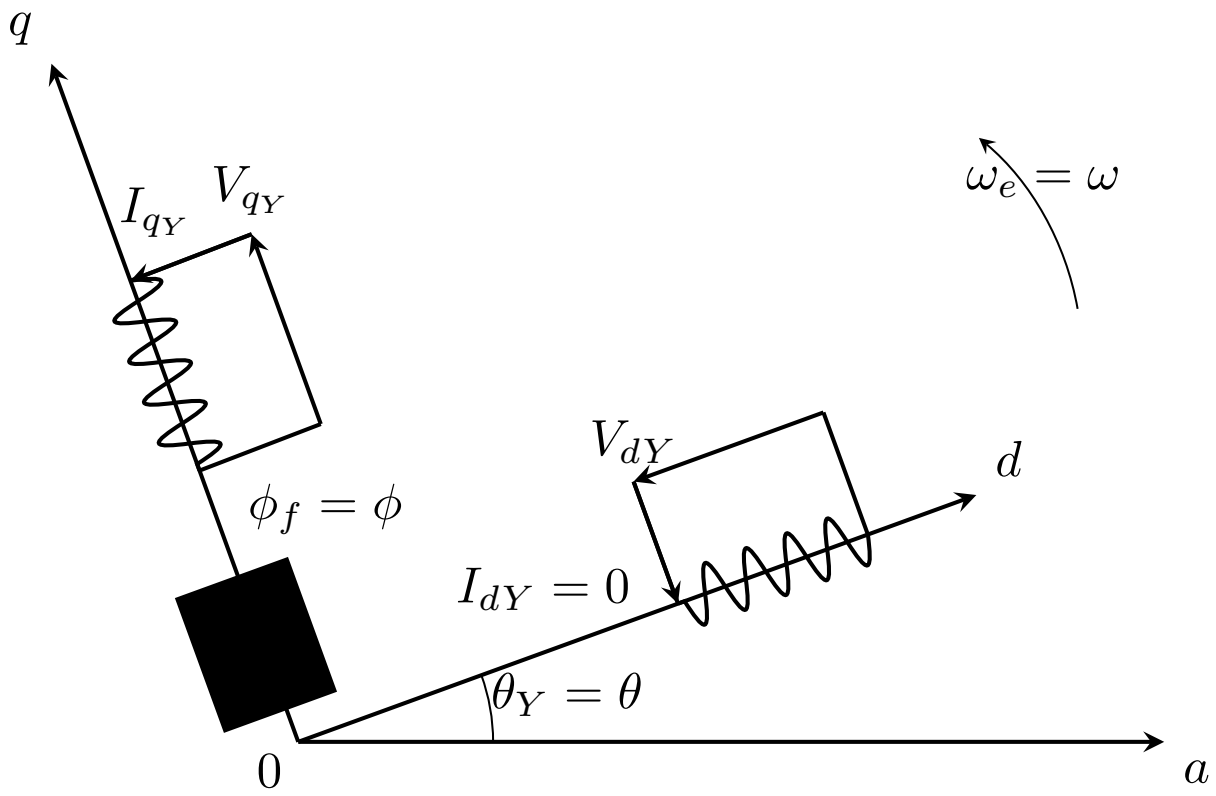

Fig. 3: Rotating two-phase reference frame.

c) Reference Frame Synchronized with the Rotating Field:

In this reference frame, the d and q axes remain fixed with respect to the rotating magnetic field generated by the stator windings. It is commonly used in control strategies because electrical quantities become steady (constant in steady state), which simplifies analysis and regulation [1].

3) Model of the DS-PMSM in the (d, q) Reference Frame:

$$\varphi_{q_Y}^{PM}(t) = 0$$

With the transformation from (1), the system then becomes:

$$\begin{cases} \varphi_{d_Y}(t) = L_{d_Y}\, i_{d_Y}(t) + \varphi(t) & \text{(11a)} \\ \varphi_{q_Y}(t) = L_{q_Y}\, i_{q_Y}(t) & \text{(11b)} \end{cases}$$

Coriolis transport formula: $\dfrac{dx_{dq}}{dt} = \dfrac{dx}{dt}_{\text{fixe}} - \omega \times x$. Thus, the voltage equations (2) in (d, q) become:

$$\begin{cases} v_{d_Y}(t) = Ri_{d_Y}(t) + \dfrac{d\varphi_{d_Y}(t)}{dt} - \omega(t)\varphi_{q_Y}(t) & \text{(12a)} \\ v_{q_Y}(t) = Ri_{q_Y}(t) + \dfrac{d\varphi_{q_Y}(t)}{dt} + \omega(t)\varphi_{d_Y}(t) & \text{(12b)} \end{cases}$$

By substitution:

$$\begin{cases} v_{dY}(t) = R_s i_{dY}(t) + L_{dY}\dfrac{di_{dY}(t)}{dt} - \omega(t) L_{qY} i_{qY}(t) \\ v_{qY}(t) = R_s i_{qY}(t) + L_{qY}\dfrac{di_{qY}(t)}{dt} + \omega(t) L_{dY} i_{dY}(t) + \omega(t)\,\varphi \end{cases} \tag{13}$$

4) State Equations of the DS-PMSM in the (d, q) Frame:

The overall system behavior can be described by equations (5), (6) and (13).

$$\begin{cases} \dfrac{di_{d_Y}(t)}{dt} = \dfrac{1}{L}[v_{d_Y}(t) - R i_{d_Y}(t) + \omega(t) L i_{q_Y}(t)] \\ \dfrac{di_{q_Y}(t)}{dt} = \dfrac{1}{L}[v_{q_Y}(t) - R i_{q_Y}(t) - \omega(t) L i_{d_Y}(t) - \omega(t)\varphi] \\ C_{em}(t) = n_{pp}\,\varphi\,(i_{qA}(t) + i_{qB}(t)) \\ J\dfrac{d\omega_{mec}(t)}{dt} = C_{em}(t) - C_r(t) - f\,\omega_{mec}(t) \end{cases}$$

IV. Modeling of the Static Converter

A. Simplifying Assumptions

- Behavioral and non-physical model: no modeling of IGBTs nor two-level switching [13].
- Single DC supply V_{dc} shared by both inverters [14] [15].
- Sinusoidal-triangular PWM identical for each phase [14].
- Triangular carrier with period T, symmetric and perfectly linear [16].
- Balanced three-phase systems without neutral [17].
- Ideal comparators, without dead time [18].

B. PWM Logic Signal Generation

For each star $Y \in \{\text{A,B}\}$ and each phase $i \in \{1, 2, 3\}$:

$$S_{Y_i}(t) = \begin{cases} 1, & V^{\star}_{Y_i}(t) > V_{\text{tri}}(t) \\ 0, & \text{otherwise} \end{cases}$$

with

$$V_{\text{tri}}(t) = \begin{cases} -\dfrac{4V_{\text{pmax}}}{T}t + V_{\text{pmax}}, & 0 \le t < T/2 \\ \dfrac{4V_{\text{pmax}}}{T}t - 3V_{\text{pmax}}, & T/2 \le t \le T \end{cases}$$

$$[-V_{\text{pmax}}, +V_{\text{pmax}}] = \left[-\frac{V_{\text{dc}}}{3}, +\frac{V_{\text{dc}}}{3}\right]$$

C. Reconstruction of Phase Voltages (Logical Model)

$$\vec{V}_Y(t) = \frac{V_{\text{dc}}}{3}\begin{bmatrix} 2 & -1 & -1 \\ -1 & 2 & -1 \\ -1 & -1 & 2 \end{bmatrix} \cdot \vec{S}_Y(t)$$

$$\vec{S}_Y^{\top} = \begin{bmatrix} S_{Y1} & S_{Y2} & S_{Y3} \end{bmatrix}$$

D. Full Summary of the Behavioral Model for the Dual-Inverter DS-PMSM

$$S_{X_i}(t) = \begin{cases} 1, & V^{*}_{X_i}(t) > V_{\text{tri}}(t) \\ 0, & \text{otherwise} \end{cases}$$

$$\vec{V}_X(t) = \frac{V_{\text{dc}}}{3}\begin{bmatrix} 2 & -1 & -1 \\ -1 & 2 & -1 \\ -1 & -1 & 2 \end{bmatrix} \vec{S}_X(t)$$

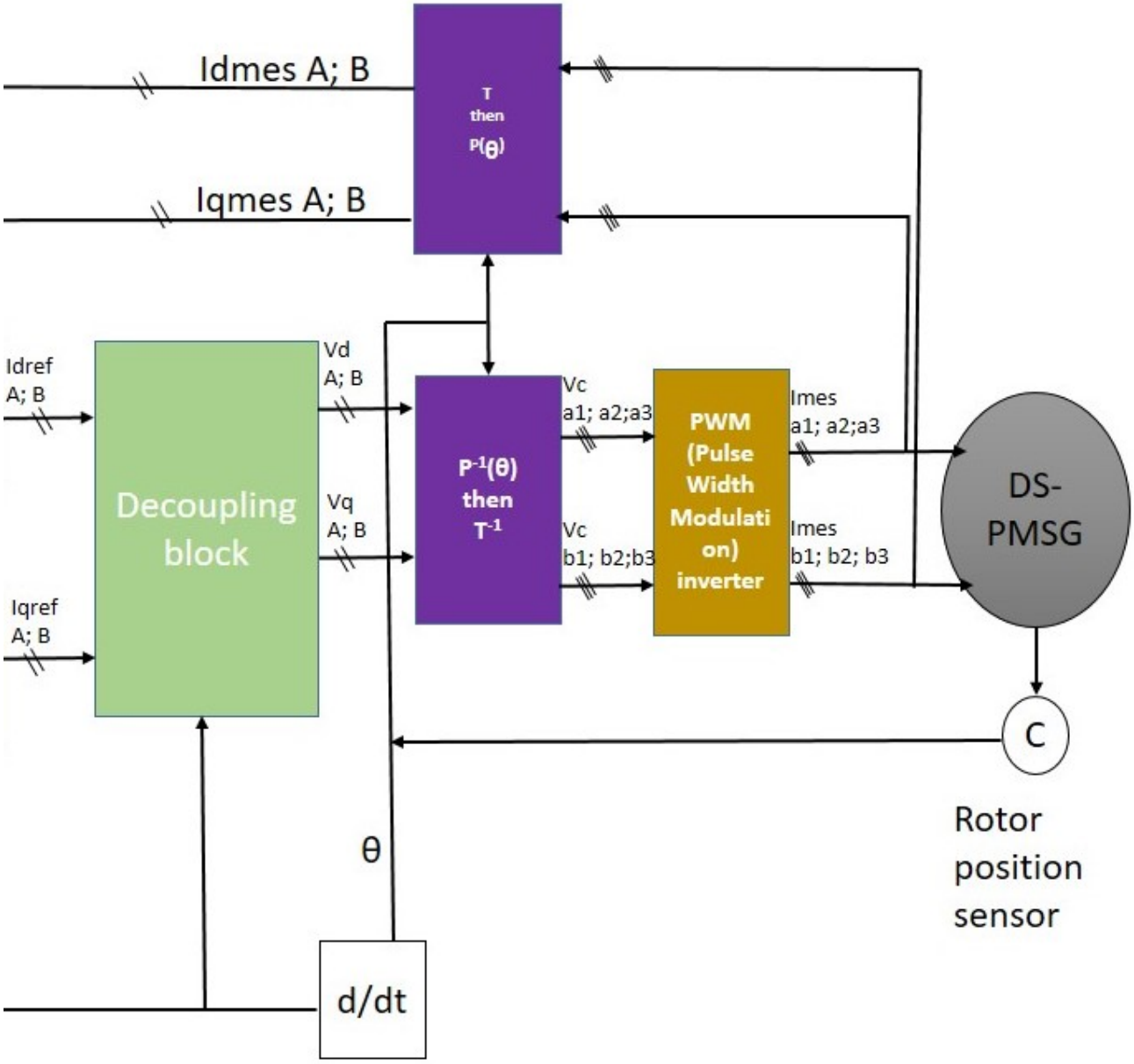

Fig. 4: Model of the DS-PMSM with the converter, decoupling block, and $\alpha\beta \leftrightarrow dq$ transformations.

V. Simulations and Results

The diagrams below show the overall representation of the associated machine and static converter, as implemented in the simulation environment.

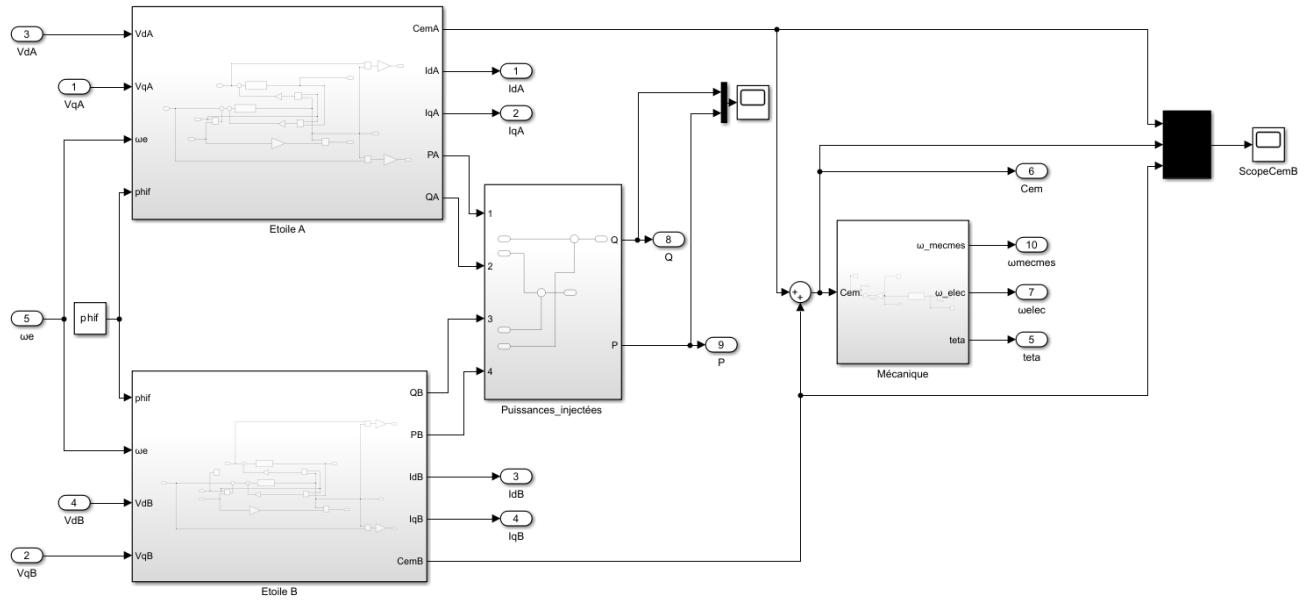

Fig. 5: Global view of the Simulink model of the double-star permanent magnet synchronous machine (DS-PMSM) coupled with the mechanical block and the calculation of injected powers

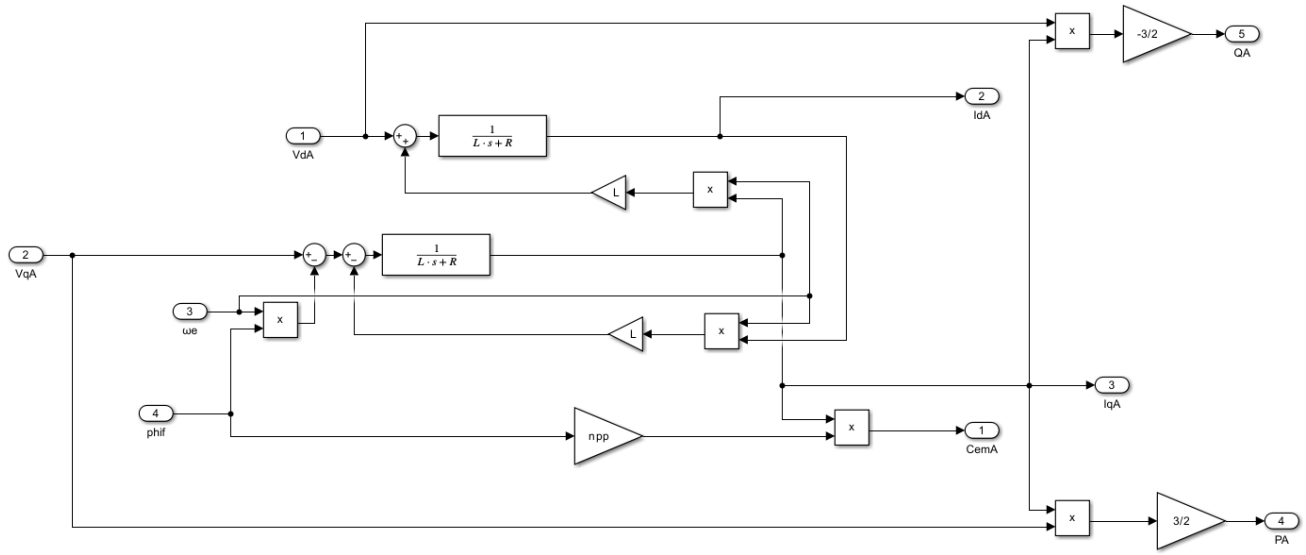

Fig. 6: Simulink model of the *Star A* subsystem of the DS-PMSM, representing the dynamic equations in the reference frame (d, q) and the calculation of electromagnetic powers and torque.

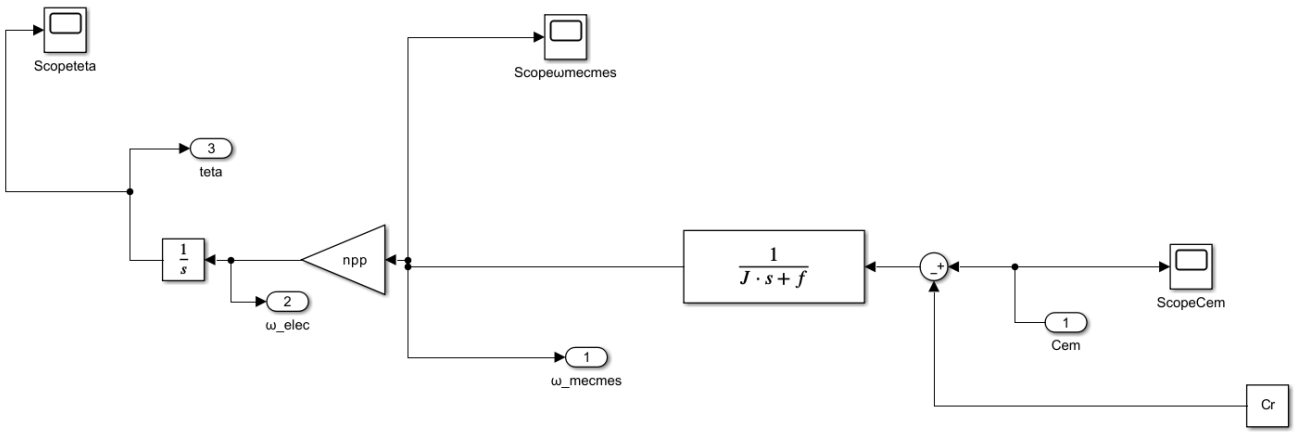

Fig. 7: Simulink model of the *Mécanique* subsystem of the DS-PMSM, illustrating the rotor dynamics according to the mechanical equation

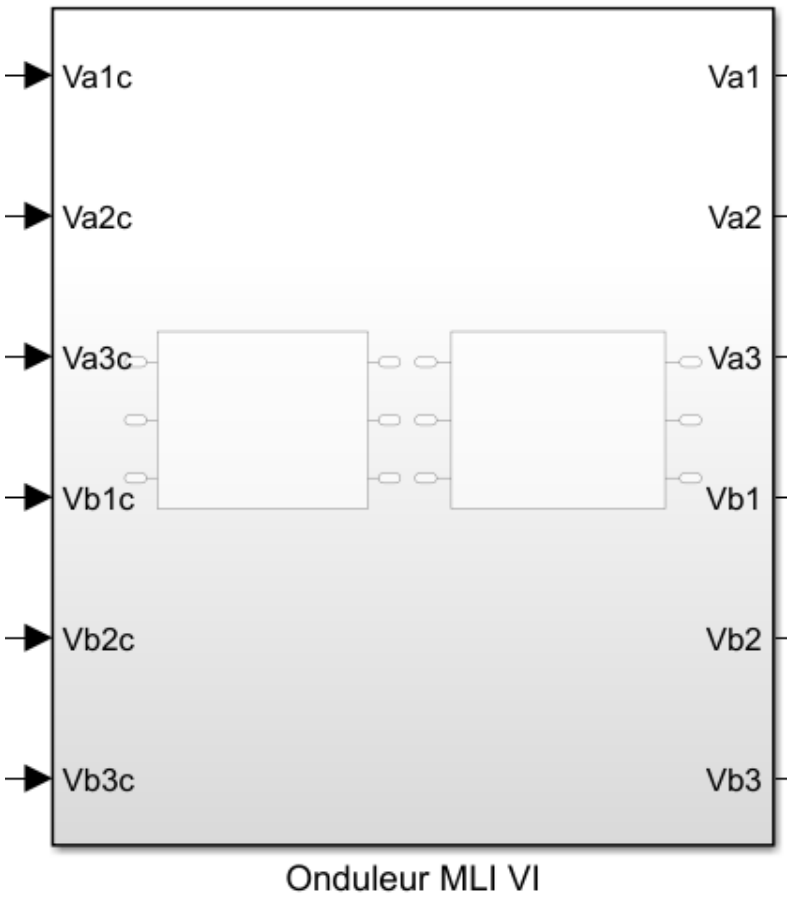

Fig. 8: Simulink model of the MLI VI inverter, ensuring continuous–alternative conversion for the two three-phase sets of the DS-PMSM.

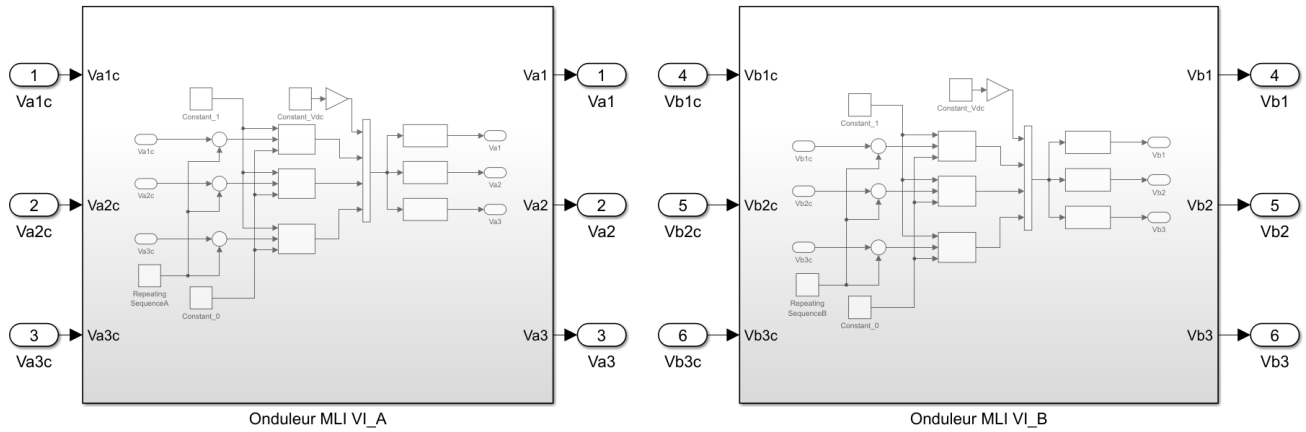

Fig. 9: Simulink model of the two inverter subsystems textitMLI VI _A and *MLI VI _B*, ensuring energy conversion for the two three-phase sets of the permanent magnet double star synchronous machine (DS-PMSM).

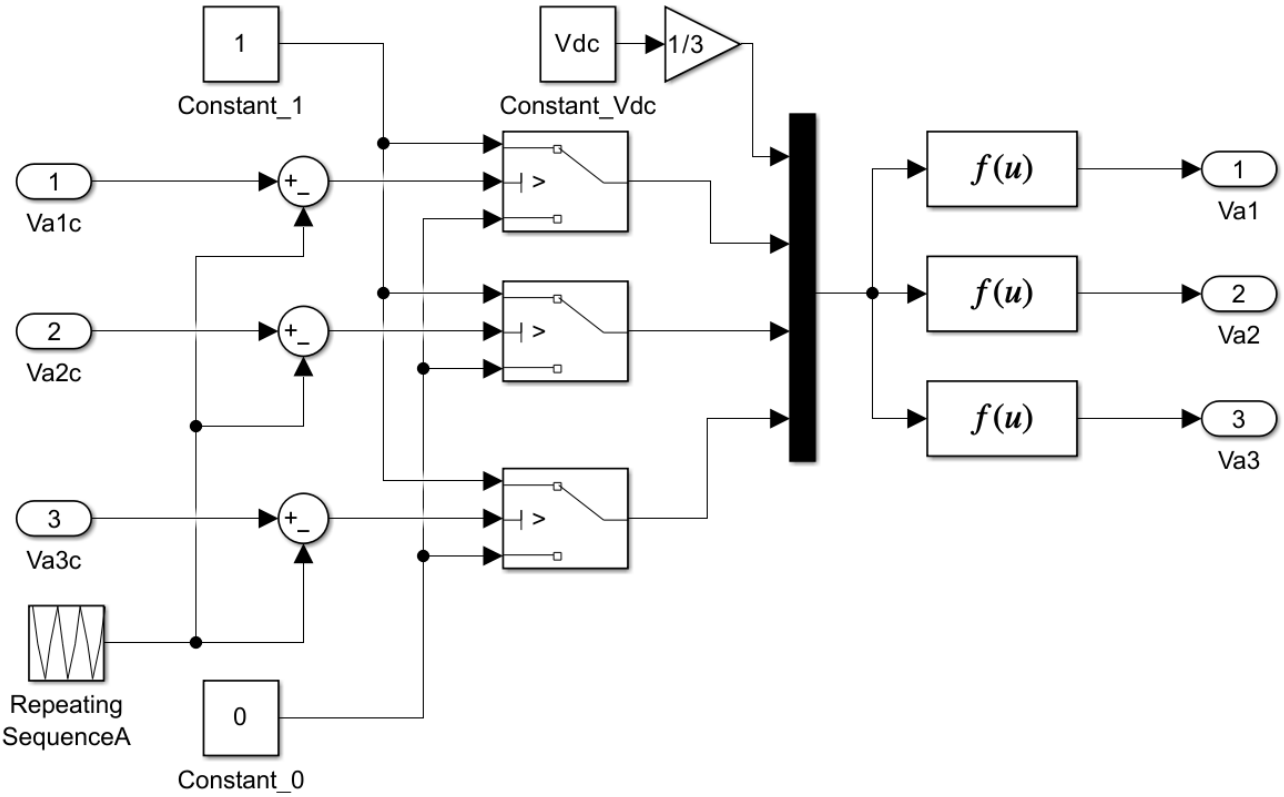

Fig. 10: Simulink model of the inverter *MLI VI _A*, illustrating the generation of control signals and the formation of three-phase output voltages (V_{a1}, V_{a2}, V_{a3}) from the comparison between the triangular carrier and the modulation signals.

The simulation is carried out using the data provided in the table below:

Parameter	**Symbol**	**Typical Value**	**Unit**
Stator resistance	$R_s = R$	0.013	Ω
d- and q-axis inductance	$L_d = L_q = L$	8.5	mH
PM rotor flux	$\varphi^{PM} = \phi$	0.119	Wb
Mechanical inertia	J	0.0027	kg·m^2
Viscous friction coefficient	f	0.000492	N·m·s/rad
Reference mechanical speed	ω_{mecref}	314	rad/s
Number of pole pairs	n_{pp}	4	–

TABLE I: Physical and electromagnetic parameters of the DS-PMSM.

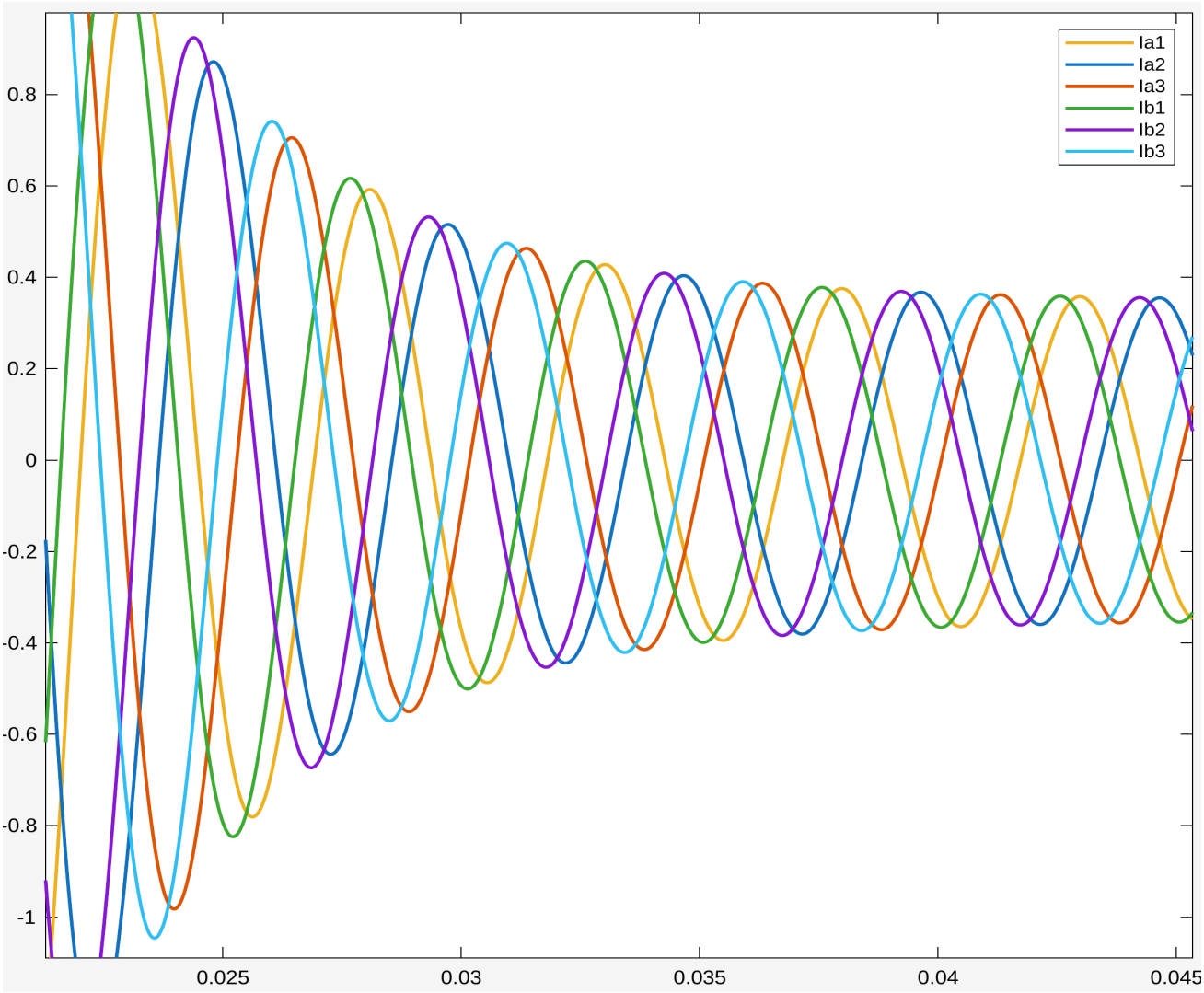

Fig. 11: Time evolution of the three-phase stator currents under balanced conditions.

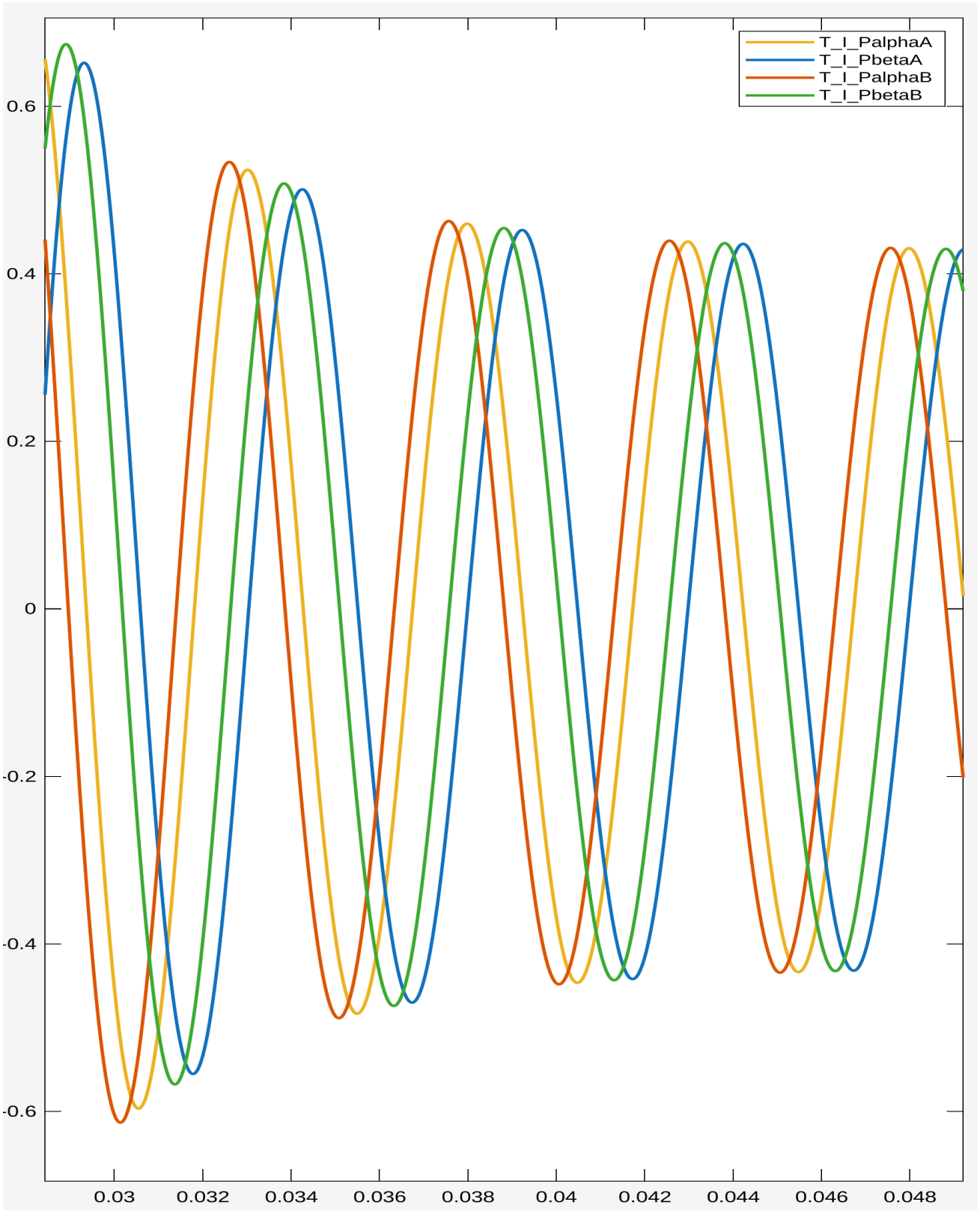

Fig. 12: Alpha and beta components of the transformed stator currents (stars A and B).

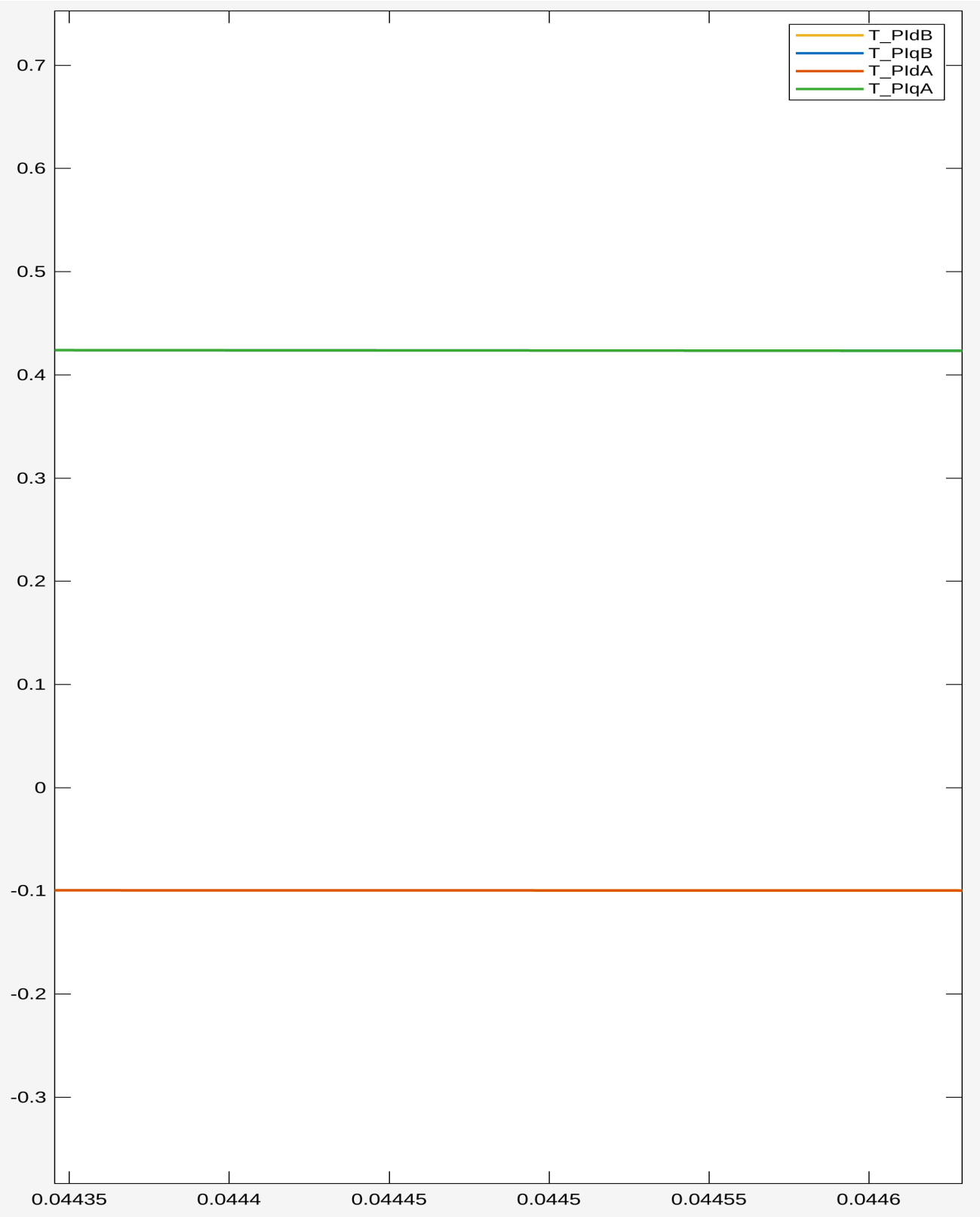

Fig. 13: Direct-axis (i_d) and quadrature-axis (i_q) currents in steady state for both stator stars.

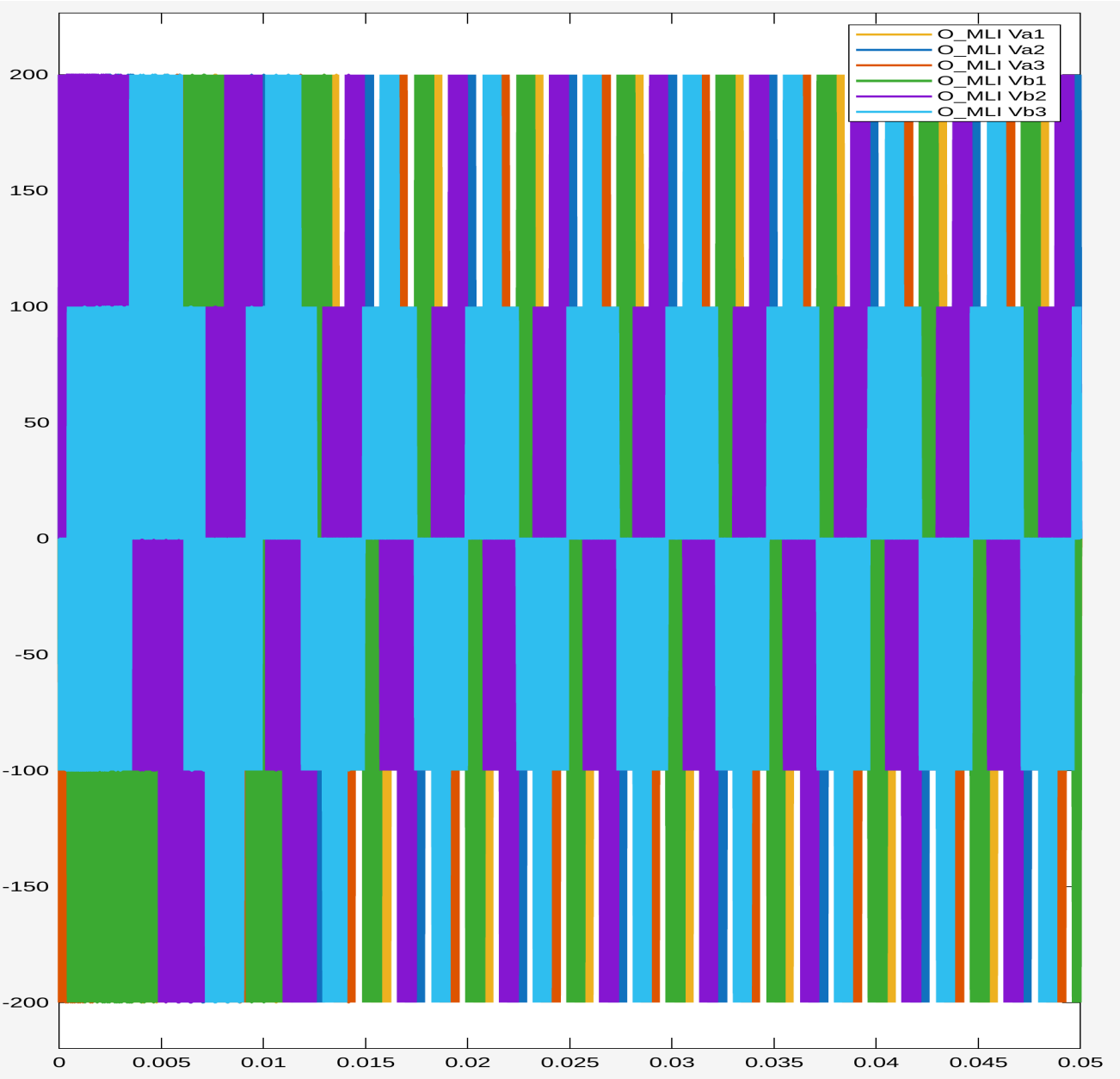

Fig. 14: Control voltages from PWM inverters for both stator stars.

VI. Discussion

The proposed modeling enables a deep understanding of the interactions between the machine and its converter. It provides a solid foundation for the implementation of vector control (FOC), predictive control (MPC), or DTC strategies. However, the lack of consideration for losses and nonlinearities may limit the model's accuracy in extreme operating conditions.

VII. Conclusion and Perspectives

This work establishes a consistent and rigorous model of the Double-Star Permanent Magnet Synchronous Machine (DS-PMSM) and its conversion interface, based on classical transformations and coupled electromechanical dynamics. Future steps will include the integration of P/Q regulation, fault consideration, and experimental validation of the model.

REFERENCES

[1] S. Kallio, M. Andriollo, A. Tortella, and J. Karttunen, "Decoupled d-q model of double-star interior-permanent-magnet synchronous machines," *IEEE Transactions on Industrial Electronics*, vol. 60, no. 6, pp. 2486–2494, Jun. 2013. DOI: 10.1109/TIE.2012.2216241.

[2] E. Amirouche, L. Kaci, G. Kaci, and D. Aouzellag, "Simulation study of the dual star permanent magnet synchronous machine using different modeling approaches," in *Proceedings of the 4th International Conference on Electrical Engineering and Control Applications (ICEECA 2019)*, ser. Lecture Notes in Electrical Engineering, S. Bououden, M. Chadli, S. Ziani, and I. Zelinka, Eds., vol. 682, Singapore: Springer, 2021. DOI: 10.1007/978-981-15-6403-1_27.

[3] M. Andriollo, G. Bettanini, G. Martinelli, A. Morini, and A. Tortella, "Analysis of double-star permanent-magnet synchronous generators by a general decoupled d–q model," *IEEE Transactions on Industry Applications*, vol. 45, no. 4, pp. 1416–1424, Jul. 2009. DOI: 10.1109/TIA.2009.2023553.

[4] N. Maakouf and A. Naami. "Commande vectorielle de la machine synchrone double étoile alimentée par deux onduleurs multicellulaires à cinq niveaux." Mémoire d'ingénieur (PFE), École Nationale Polytechnique (ENP), Alger, Algérie. [Online]. Available: https://repository.enp.edu.dz/xmlui/handle/123456789/3677.

[5] E. Amirouche, K. Iffouzar, A. Houari, K. Ghedamsi, and D. Aouzellag, "Improved control strategy of dual star permanent magnet synchronous generator based tidal turbine system using sensorless field oriented control and direct power control techniques," *Energy Sources, Part A: Recovery, Utilization, and Environmental Effects*, vol. 47, no. 1, pp. 5986–6007, 2021. DOI: 10.1080/15567036.2021.1902429.

[6] I. Abdulwahab, A. S. Abubakar, A. Olaniyan, B. O. Sadiq, and S. A. Faskari, "Control of dual stator induction generator based wind energy conversion system," in *2022 IEEE Nigeria 4th International Conference on Disruptive Technologies for Sustainable Development (NIGERCON)*, Lagos, Nigeria, 2022, pp. 1–5. DOI: 10.1109/NIGERCON54645.2022.9803100.

[7] A. G. Yepes, I. Gonzalez-Prieto, O. Lopez, M. J. Duran, and J. Doval-Gandoy, "A comprehensive survey on fault tolerance in multiphase ac drives, part 2: Phase and switch open-circuit faults," *Machines*, vol. 10, no. 3, p. 221, 2022. DOI: 10.3390/machines10030221.

[8] J. Li, "Characteristics of synchronous generator," in *Design and Application of Modern Synchronous Generator Excitation Systems*, Wiley, 2019. DOI: 10.1002/9781118841006.ch2.

[9] C. Liu, "Emerging electric machines and drives — an overview," *IEEE Transactions on Energy Conversion*, vol. 33, no. 4, pp. 2270–2280, Dec. 2018. DOI: 10.1109/TEC.2018.2852732.

[10] J. R. Chapman, *Electric Machinery Fundamentals*, 5th. New York, NY, USA: McGraw-Hill, 2011, ISBN: 978-0-07-352954-7.

[11] S. Asfirane, S. Hlioui, Y. Amara, and M. Gabsi, "Study of a hybrid excitation synchronous machine: Modeling and experimental validation," *Mathematical and Computational Applications*, vol. 24, no. 2, p. 34, 2019. DOI: 10.3390/mca24020034.

[12] S. Hlioui, Y. Amara, M. Gabsi, et al., "Hybrid excited synchronous machines," *IEEE Transactions on Magnetics*, vol. 58, no. 2, pp. 1–10, Feb. 2022, Art no. 8101610. DOI: 10.1109/TMAG.2021.3079228.

[13] Z. Zhu, S. Wang, B. Shao, L. Yan, P. Xu, and Y. Ren, "Advances in dual-three-phase permanent magnet synchronous machines and control techniques," *Energies*, vol. 14, no. 22, p. 7508, 2021. DOI: 10.3390/en14227508.

[14] J.-Y. Zhang, Q. Zhou, and K. Wang, "Dual three-phase permanent magnet synchronous machines vector control based on triple rotating reference frame," *Energies*, vol. 15, no. 19, p. 7286, 2022. DOI: 10.3390/en15197286.

[15] I. K. Iparragirre, E. I. Basabe, A. M. S. González, and A. Navarro-Temoche, "Modelling and simulation of dual three-phase pmsms on the phase variable reference frame," in *Proceedings of the XXX Seminario Anual de Automática, Electrónica Industrial e Instrumentación (SAAEI'23)*, [Online]. Available: http://hdl.handle.net/10810/68872, 2023.

[16] J. Karttunen, S. Kallio, P. Peltoniemi, P. Silventoinen, and O. Pyrhönen, "Decoupled vector control scheme for dual three-phase permanent magnet synchronous machines," *IEEE Transactions on Industrial Electronics*, vol. 61, no. 5, pp. 2185–2196, May 2014. DOI: 10.1109/TIE.2013.2270219.

[17] E. Levi, R. Bojoi, F. Profumo, H. A. Toliyat, and S. Williamson, "Multiphase induction motor drives—technology status and future trends," *IET Electric Power Applications*, vol. 1, no. 4, pp. 489–516, Jul. 2007. DOI: 10.1049/iet-epa:20060342.

[18] A. Hassan, X. Yang, W. Chen, and M. A. Houran, "A state of the art of the multilevel inverters with reduced count components," *Electronics*, vol. 9, no. 11, p. 1924, 2020. DOI: 10.3390/electronics9111924.